

The Isotopic Mixture of Barium in the Metal-poor Subgiant HD 140283

David L. Lambert and Carlos Allende Prieto

Department of Astronomy, University of Texas, Austin, TX 78712-1083, USA

Accepted . Received ; in original form 2002

ABSTRACT

Analyses of the abundances of neutron-capture elements have led to the belief that these elements in metal-poor stars are r -process products with relative abundances closely resembling those found in the solar system. This picture was challenged by Magain (1995), who found that a pure r -process mix of the barium isotopes was inconsistent with the mix of odd to even barium isotopes derived from analysis of the Ba II line at 4554 Å in the spectrum of the metal-poor subgiant HD 140283. In this paper, we address Magain’s challenge using new high resolution high signal-to-noise spectra of HD 140283, and find, in contrast to his result, that a solar-like r -process isotopic mixture provides a fair fit to the observed 4554 Å profile.

Key words: Star: individual: HD 140283:

1 INTRODUCTION

Nucleosynthesis of heavy elements is dominated by the two neutron-capture processes known as the s - and the r -process. Some nuclides can be synthesized by only the s -process, and others by only the r -process. Both processes contribute almost all the remaining nuclides, with the exception of a few heavy neutron-poor nuclides of low abundance termed p -nuclei, which cannot be synthesized by either process.

The He-shell of a star in the asymptotic giant branch (AGB) has been identified as the site responsible for the *main* s -process, which synthesizes nuclides heavier than about strontium. Of the observable elements, barium and heavier elements are to differing degrees produced through the *main* s -process. What is known as the *weak* s -process synthesizes nuclides between the iron-group elements and about strontium. Operation of the *weak* s -process is considered to occur in the helium and carbon shells of massive stars in their hydrostatic burning phases. The r -process is likely associated with the deep interior of Type II supernovae.

Since massive stars dying as Type II supernovae evolve faster than the stars that populate and evolve from the AGB, one anticipates that very metal-poor stars, formed from the interstellar medium (ISM) when it was little polluted with stellar ejecta, will contain r -process products but little to no *main* s -process products. Products of the *weak* s -process may accompany r -process products but their abundance is likely very low. As the Galaxy aged and the ISM became more polluted, the stars that formed would have contained more metals and both r - and s -process products. In this

picture, one expects the heavy elements in the most metal-poor stars to be exclusively r -process products, a suggestion made by Truran (1981).

Magain (1995, see also Magain & Zhao 1993a) claimed, on the basis of published elemental abundances, that “there is no secure observational evidence in support of Truran’s suggestion”. He applied a novel test to the metal-poor subgiant HD 140283 to determine the relative contributions of the r - and s -process, and used the result to reinforce his claim. His test, which had been anticipated by Cowley & Frey (1989), involved an analysis of the Ba II 4554 Å line profile to determine the fractional abundance of the odd isotopes. Contributions of the various isotopes cannot be distinguished in the 4554 Å line’s profile solely on the basis of the very small isotopic wavelength shifts, but the hyperfine splittings (about -30 mÅ to + 20mÅ) contributed by the two odd isotopes result in a broadening of the stellar line that is dependent on the abundance ratio of the odd to even isotopes. According to the analyses of the solar system abundances, the s - and r -process contribute quite differently to the fractional abundance of the odd isotopes, that is $f_{\text{odd}} = [N(^{135}\text{Ba}) + N(^{137}\text{Ba})]/N(\text{Ba})$ where $f_{\text{odd}}^s = 0.11$ but $f_{\text{odd}}^r = 0.46$, according to Arlandini et al. (1999). Thus, the line width, which offers a way to measure f_{odd} , is a potential indicator of the relative contributions of the s - and r -process.

Magain obtained and analysed a high-resolution ($R \equiv \lambda/\Delta\lambda = 100,000$) high signal-to-noise ($S/N \simeq 400$) observation of the 4554 Å line in the spectrum of HD 140283. Using the Fe II line at 4555.9 Å to determine the broaden-

arXiv:astro-ph/0205376v1 22 May 2002

ing of a line unaffected by isotopic and hyperfine splitting, Magain’s fit to the 4554 Å line gave the fractional abundance of the odd Ba isotopes as $f_{\text{odd}} = 0.06 \pm 0.06$. On the basis of the solar estimates of f_{odd}^s and f_{odd}^r , Magain concluded that HD 140283’s barium isotopic ratio reflects ‘pure *s*-process production’ and ‘significant enhancement of the *r*-process contribution’ is excluded. This conclusion reinforced his critique of published abundance analyses of metal-poor stars.

In this paper, we reobserve and analyse afresh HD 140283’s Ba II 4554 Å line profile. Our new spectra, superior to the material previously published, are described in Section 2. The isotopic analysis is discussed in Section 3, and the paper concludes with a discussion of the barium isotopic mix in the context of the heavy element composition of HD 140283 and other metal-poor stars.

2 OBSERVATIONS

All of our observations of HD 140283 were carried out with the Harlan J. Smith Telescope and the *2dcoudé* cross-dispersed echelle spectrograph (Tull et al. 1995) at the W.J. McDonald Observatory (Mt. Locke, West Texas). Spectra with a FWHM resolving power $R \simeq 200,000$ were secured on May 23-25, 1997. A series of 1/2 hour exposures were cross-correlated and combined to reach a signal-to-noise ratio ~ 550 per pixel at the Ba II line. The detector was a 2k×2k Tektronix CCD with a very large dynamic range. We refer the reader to Allende Prieto (1998) and Allende Prieto et al. (1999) for more information about these data.

Observations at a resolving power $R \simeq 60000$ and with a S/N around 200 were acquired in 1993 and 1994 by Ramón J. García López with a 1k×1k Tektronix CCD. These spectra provided equivalent widths for 64 iron lines that were used to constrain the microturbulence. Equivalent widths were measured by Gaussian fits to individual or slightly blended lines.

3 LINE PROFILE ANALYSIS

The profile of the Ba II 4554 Å line is set by isotopic and hyperfine splittings, and by physical conditions in the stellar atmosphere such as turbulent motions and the stellar rotation. We use model atmospheres and our high-resolution spectra to constrain the stellar contributions to the line profile.

The isotopic and hyperfine splittings have been measured by laboratory spectroscopists. Rutten (1978) collated the measurements. McWilliam (1998) used these data to calculate the components of the 4554 Å line (and other lines). He ignored the isotopic wavelength shifts of the even isotopes, but this is acceptable here: the $^{134}\text{Ba} - ^{138}\text{Ba}$ shift is only about 2.4 mÅ. Then, even isotopes produce the single component that we have centred, following McWilliam, at 4554.000 Å. No rational distinction can be made between the two odd isotopes. The true central wavelength is not important, given the uncertainties in the radial velocity of the star, convective motions, oscillations, etc., and we allow for a velocity shift between the observed and calculated profiles. The relative intensities of the hyperfine splitting (hfs)

Table 1. HD 140283: Results of Spectroscopic Analyses

Authors	T_{eff} (K)	$\log g$ (cgs)	[Fe/H]	[Sr/Fe]	[Y/Fe]	[Ba/Fe]	[Eu/Fe]
MMZ ^a	5640	3.10	-2.8	-0.34	-0.58	-1.13	+0.21
GS ^b	5690	3.58	-2.6	-0.03	-0.38	-0.64	+0.09
RNB ^c	5750	3.40	-2.5	-0.44	+0.18	-0.91	...
MGB ^d	5640	3.65	-2.3	-0.80	...
F ^e	5650	3.40	-2.4	-1.03	...
MK ^f	5650	3.5	-2.4	...	-0.19	-0.78	...
LAP ^g	5777	3.74	-2.4	-1.09	...

^a Magain (1989) and Magain & Zhao (1990): also [La/Fe] = -0.05

^b Gratton & Sneden (1994)

^c Ryan, Norris, & Beers (1996)

^d Mashonkina, Gehren, & Bikmaev (1999)

^e Fulbright (2000)

^f Mishenina & Kovtyukh (2001)

^g This paper

components of the 4554 Å line published by McWilliam are in good agreement with the calculation of Cowley & Frey (1989) and our own. (We adopt McWilliam’s choice for the line’s *gf*-value [$\log gf = +0.17$].)

Our analysis used a classical model atmosphere constructed for the standard assumptions of plane parallel homogeneous layers in hydrostatic, flux, and local thermodynamic equilibrium. The model was taken from the Kurucz (1992) grid of non-overshooting models. By interpolation, we obtained a model atmosphere for the parameters: $T_{\text{eff}} = 5777$ K, $\log g = 3.74$, and [Fe/H] = -2.7, which are very similar to the values recommended by Snider et al. (2001) based on the Infrared flux method and the parallax measured by *Hipparcos*. In Table 1, we list the adopted parameters and the abundances found in some of the previous analyses. Our metallicity in Table 1 corresponds to the iron abundance we derive below, scaled to the solar value we find from a parallel analysis of the solar flux spectrum of Kurucz et al. (1984). As pointed out by Magain (1995), the predicted Ba II line profiles are relatively insensitive to the particular choice of stellar parameters. We calculated synthetic spectra using the LTE code MOOG (Sneden 1973), and checked the results with a second LTE code MISS (Allende Prieto et al. 1998), noticing negligible differences between their outputs.

With the chosen model atmosphere, we analysed the equivalent widths of iron lines measured off the $R = 60,000$ spectra, finding that a microturbulence of $\xi = 1.42 \text{ km s}^{-1}$ made the iron abundance independent from the line equivalent width to yield $\log \epsilon(\text{Fe}) = 5.18 \pm 0.11$ from 51 Fe I lines (*gf*-values from Oxford; e.g., Blackwell et al. 1986) and $\log \epsilon(\text{Fe}) = 5.12 \pm 0.08$ (*gf*-values from Giridhar & Arellano Ferro 1994) from 13 Fe II lines. Here and subsequently, we have adopted the standard deviation (σ) as the uncertainty. The equivalent widths, atomic data, and abundances for the individual lines appear in Table 2. Note that the ionisation equilibrium of iron is rather well satisfied by this analysis.

Adopting the above microturbulence, we analysed a sample of Fe I lines observed at $R \simeq 200,000$ (see Table 3). The transition probabilities of these lines have been measured by O’Brian et al. (1991) and/or at Oxford. We achieved the best fit to the line profiles by varying the iron abundance, the central wavelength of the line, and the

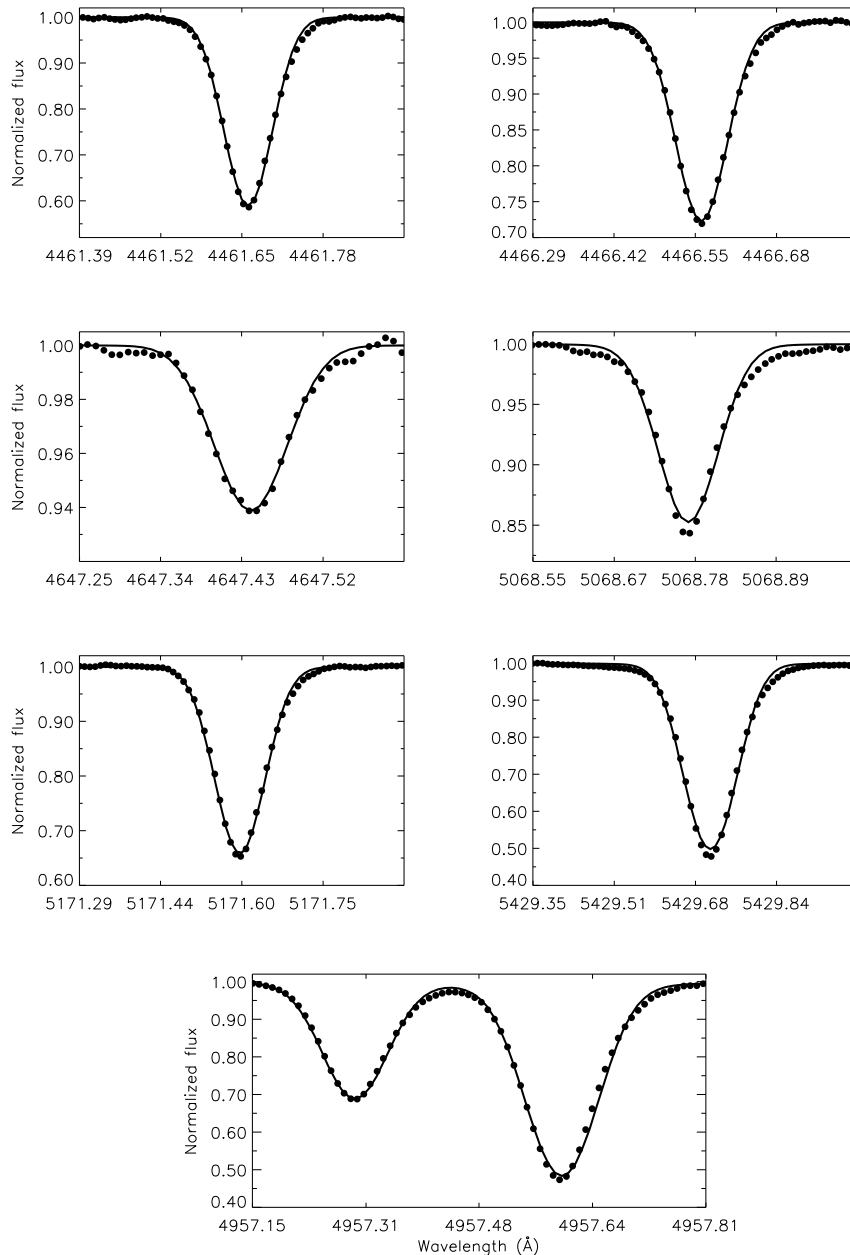


Figure 1. Best-fit synthetic profiles (thick solid) compared to the observed spectra for eight iron lines used to determine the velocity and instrumental line broadening in the spectrum of HD 140283.

FWHM of an assumed-Gaussian broadening. The Gaussian is intended to account for the rotational, macroturbulent, and instrumental broadening. Collisional broadening by hydrogen atoms is considered using the theory and parameters prescribed by Barklem, Piskunov, & O’Mara (1999), and references therein. Approximate formulae were used for the less important Stark and natural broadening. Table 3 lists the best-fitting parameters, while Fig. 1 illustrates the fitting graphically. This set of Fe I lines give $\log \epsilon(\text{Fe}) = 5.09 \pm 0.09$, and a FWHM of $5.06 \pm 0.33 \text{ km s}^{-1}$ for the Gaussian broadening. A fit to the Fe II line used by Magain gives $\text{FWHM} = 5.5 \text{ km s}^{-1}$, a value within the scatter of results from the Fe I lines. The fits were accomplished by the Nelder-Mead

simplex method (Nelder & Mead 1965), as implemented by Press et al. (1988). It is interesting to note that we obtain a consistent iron abundance from the analysis of the equivalent widths in Table 3, which were measured by fitting a Gaussian to the observed profiles. Replacing the damping parameters calculated by Barklem et al. (1999) by the Unsöld approximation, our abundance estimate would increase by 0.04 dex.

Next, we fit the profile of the Ba II 4554 Å line by changing the barium abundance, and f_{odd} . Our ultra-high resolution spectra can easily distinguish the effects of the two parameters; at the metallicity of HD 140283, the equivalent width is almost independent of f_{odd} . We found that a linear

Table 2. Spectral Lines Selected to determine the microturbulence in HD 140283

Wavelength (Å)	EP (eV)	log gf (dex)	W_λ (mÅ)	log $\epsilon(\text{Fe})$ (dex)
Fe I				
3786.68	1.01	-2.23	40	5.18
3790.10	0.99	-1.76	54	5.05
3833.31	2.56	-1.03	20	5.02
3906.48	0.11	-2.24	79	5.42
3917.18	0.99	-2.16	44	5.17
4005.25	1.56	-0.61	79	5.24
4067.27	2.56	-1.42	11	5.07
4147.67	1.49	-2.10	24	5.11
4152.17	0.96	-3.23	9	5.18
4172.75	0.96	-3.07	16	5.29
4174.92	0.92	-2.97	16	5.15
4177.60	0.92	-3.06	24	5.50
4202.03	1.49	-0.71	78	5.18
4216.19	0.00	-3.36	39	5.21
4222.22	2.45	-0.97	31	5.08
4250.12	2.47	-0.41	52	5.06
4271.16	2.45	-0.35	60	5.17
4337.05	1.56	-1.70	35	5.03
4375.93	0.00	-3.03	55	5.24
4442.34	2.20	-1.26	30	5.10
4447.72	2.22	-1.34	25	5.07
4489.74	0.12	-3.97	11	5.15
4494.57	2.20	-1.14	34	5.08
4733.60	1.49	-2.99	6	5.18
4939.69	0.86	-3.34	10	5.16
4994.13	0.92	-3.08	14	5.13
5012.07	0.86	-2.64	32	5.13
5079.23	2.20	-2.07	9	5.19
5079.74	0.99	-3.22	13	5.29
5083.34	0.96	-2.96	16	5.10
5107.45	0.99	-3.09	12	5.13
5107.65	1.56	-2.42	14	5.10
5110.41	0.00	-3.76	25	5.20
5123.72	1.01	-3.07	12	5.14
5151.91	1.01	-3.32	7	5.11
5194.94	1.56	-2.09	26	5.13
5198.71	2.22	-2.14	9	5.24
5307.36	1.61	-2.99	6	5.31
5397.13	0.92	-1.99	64	5.26
5405.78	0.99	-1.84	67	5.24
5429.70	0.96	-1.88	68	5.29
5434.53	1.01	-2.12	53	5.18
5701.55	2.56	-2.22	3	5.06
6065.49	2.61	-1.53	10	5.04
6136.62	2.45	-1.40	20	5.11
6137.70	2.59	-1.40	17	5.16
6219.29	2.20	-2.43	3	4.99
6252.56	2.40	-1.69	14	5.17
6265.14	2.18	-2.55	5	5.29
6593.88	2.43	-2.42	6	5.44
6750.15	2.42	-2.62	3	5.36
Fe II				
4173.49	2.58	-2.18	27	5.02
4178.86	2.58	-2.48	20	5.14
4489.19	2.82	-2.96	5	5.13
4491.41	2.85	-2.70	8	5.10
4555.90	2.83	-2.29	17	5.06
4303.17	2.70	-2.49	19	5.22
4416.83	2.77	-2.55	11	5.05
4583.85	2.80	-1.84	42	5.19
4731.46	2.89	-2.92	4	5.03
4923.93	2.89	-1.24	57	5.01
5234.64	3.22	-2.24	13	5.22
5316.62	3.15	-1.85	24	5.10
6456.40	3.90	-2.20	4	5.22

relationship of the form $f_{\text{odd}} = 0.51 - 0.51(\text{FWHM} - 4.65)$ represents very well the dependence of the derived f_{odd} on the magnitude of the Gaussian broadening. For $\text{FWHM} = 5.06 \pm 0.33 \text{ km s}^{-1}$, we find our best fit (reduced $\chi^2 = 2.9$) with $\log \epsilon(\text{Ba}) = -1.18 \pm 0.02 \text{ dex}$ and $f_{\text{odd}} = 0.30 \pm 0.17$. Note that our FWHM for the Fe II line used by Magain would give a value of $f_{\text{odd}} (\simeq 0.08)$ close to his value. The FWHM of the Ba II line appears not to be affected by blending lines. Cowley & Frey searched for potential blends that might be disturbing the profile in a solar-like star, concluding that only two transitions Cr I 4553.94 Å and Zr II 4553.97 Å were likely to affect the barium resonance line. Our test calculation using the atomic parameters in Kurucz's library of lines shows that these two features are irrelevant in the case of HD 140283; even if the gf -values are increased by an order of magnitude the pair together cannot contribute more than 0.1 mÅ, or about 0.5 % of the equivalent width of the barium line. Our Ba abundance is derived assuming LTE but non-LTE calculations by Mashonkina, Gehren, & Bikmaev (1999) show that the non-LTE abundance will not be very different.

The best-fit to the observed profile is shown in Fig. 2. The differences between the observed and fitted profile are symmetric about the line's centre. Using Magain's hfs model, the result for f_{odd} does not change significantly. Apart from the uncertainty in FWHM, there are other contributors to the error budget for f_{odd} . As the star is very metal-poor and the quality of the spectrum is very high, we deem the continuum determination to be reliable. If we adopt the 1σ uncertainty for $S/N = 550$, which is 0.002, this factor can alter the derived f_{odd} by no more than 0.05. Changes in T_{eff} and $[\text{Fe}/\text{H}]$ in the adopted model atmosphere can shift the barium abundance significantly, but they have no effect on f_{odd} . The adopted microturbulence is relevant: a change of $\pm 0.2 \text{ km s}^{-1}$ changes f_{odd} by ∓ 0.11 . The adopted gravity enters into the determination of f_{odd} through the pressure broadening of the line, but a variation of 0.2 dex in $\log g$, which can be taken as a conservative estimate for HD 140283, shifts f_{odd} by only 0.01. This error source should be further reduced by our procedure of fitting FWHM with a set of lines observed simultaneously and modelled with the same model atmosphere. In summary, we assign an uncertainty of about $\sqrt{0.17^2 + 0.05^2 + 0.11^2 + 0.01^2} \simeq 0.21$ to our determination of f_{odd} .

Several potential sources of error have been considered, but there are more caveats. Velocity fields might introduce differences between the FWHM of the comparison Fe I lines and the Ba II line. The set of Fe I lines spans a range of equivalent widths; some are weaker but most are slightly stronger than the barium line (20 mÅ). Our data, however, does not show a correlation of FWHM with line strength. Interestingly, Ryan et al. (2002) have recently reported correlations between line width and equivalent width for Fe I lines in metal-poor stellar spectra, in the sense that stronger lines are wider. The correlation was demonstrated for lines stronger than 30 mÅ. In the hypothetical case that such a pattern were present in HD 140283's lines, and that the barium line followed the same trend as the iron lines, the fact that most lines in Table 3 are stronger than the Ba II feature could induce a bias in the derived f_{odd} . Accounting for such an effect would imply a higher f_{odd} than we derive, in closer agreement with f_{odd}^r .

Table 3. Fe I spectral lines selected to determine the line broadening in HD 140283. The Fe II 4555.9 Å line used by Magain is listed last. σ_0 is the cross-section for broadening by collisions with neutral hydrogen for a velocity of the perturber $v_0 = 10^4$ m s $^{-1}$, and $\sigma(v) \propto v^\alpha$ (see, e.g., Barklem & O’Mara 1997).

Wavelength (Å)	EP (eV)	log gf (dex)	σ_0 (a $_0^2$)	α	FWHM (km s $^{-1}$)	log ϵ (Fe) (dex)	W_λ (mÅ)	reduced χ^2
4461.66	0.087	-3.19	217	0.250	4.7	5.12	41	10.5
4466.56	2.831	-0.60	222	0.263	5.1	5.03	29	5.7
4647.44	2.949	-1.35	283	0.259	5.1	5.06	6	0.9
4957.30	2.851	-0.41	727	0.238	5.5	4.98	37	16.3
4957.60	2.808	+0.23	714	0.238	5.5	4.98	70	16.3
5068.77	2.940	-1.04	738	0.237	4.6	5.18	16	7.1
5171.61	1.485	-1.79	281	0.253	5.1	5.08	41	3.3
5429.71	0.958	-1.88	240	0.248	4.9	5.24	68	18.4
4555.89	2.828	-2.29	5.5	5.00	16	9.8

Close examination of the profiles of unblended lines shows that they are asymmetric, and strong lines are red-shifted relative to weak lines (Allende Prieto et al. 1999). Theoretical profiles from a classical atmosphere are necessarily symmetric and unshifted relative to one another (pressure shifts are too small to be detected). It is the convective motions associated with stellar granulation that induce the line asymmetries and shifts. Inspection of Figure 1 shows that Fe I lines are asymmetric with stronger red than blue wings. A line like the Ba II line, if free from isotopic and hyperfine splittings, would also have wings red-shifted relative to the line core. The observed line is, as Figure 2 shows, quite symmetric. We may attribute this symmetry to the combination of the asymmetry due to granulation in the presence of the odd isotopes and the asymmetry of their hyperfine splittings about line centre. It would, nonetheless, be useful to repeat the analyses of the lines using 3D hydrodynamical simulations of stellar granulation.

Another source of possible error might be linked to our use of LTE line profiles. Non-LTE calculations for Ba II line formation in classical atmospheres were presented by Mashonkina & Gehren (2000). For stars as metal-poor as HD 140283, the non-LTE Ba abundance from the 4554 Å line is slightly larger than the LTE value, i.e., the non-LTE line for a given abundance is weaker than the equivalent LTE line. In the case of HD 140283, using a model with $T_{\text{eff}} = 5640$ K, $\log g = 3.65$, and $[\text{Fe}/\text{H}] = -2.30$, Mashonkina & Gehren find the non-LTE abundance from 4554 Å to be 0.15 dex larger than the LTE abundance. Our choices for atmospheric parameters are different and will affect slightly the non-LTE correction, but it is impossible to estimate the magnitude of the change from the limited results given by Mashonkina & Gehren.

The small change in Ba abundance is not a critical factor. It is the changes in the line profile that may affect the determination of f_{odd} . The NLTE source function for the 4554 Å line is predicted to be greater than the local Planck function over the region of line formation, the number density of ground state ions is reduced below the LTE value, and the line is weakened slightly. One may suppose that the weakening is more severe at the line centre than in the wings, that is the non-LTE line assumes a larger width for a given central depth than for the comparable LTE line. If the observed line is then analysed with non-LTE line profiles, the

derived f_{odd} would be slightly smaller than that from the LTE calculations.

Effects of non-LTE on the Fe I comparison lines should also be assessed but unfortunately published predictions seem too incomplete to provide a quantitative assessment. Thévenin & Idiart (1999), who performed non-LTE calculations for iron, found the Fe abundance of HD 140283 to increase by 0.29 dex when non-LTE replaced LTE in the analysis of Fe I and Fe II lines, and the determined surface gravity was in good agreement with the *Hipparcos*-based value. The leading non-LTE effect is an overionisation of neutral iron. It is impossible from the brief published description of the calculations for HD 140283 to determine the outcome on the line profiles, but it seems likely that the non-LTE profiles are slightly shallower than their LTE equivalents, as was the case for the Ba II 4554 Å line. Since we have used six different lines, we suppose that the net effect is too small to affect the mean FWHM, although it could definitely be a major source of scatter. In addition, it is clear that Thévenin & Idiart’s calculations are not the last word on the possible departures from LTE, which may be smaller than calculated by them (Fulbright 2000; Gehren et al. 2001). Indeed, our LTE analysis using the *Hipparcos*-based gravity gives consistent abundances from the Fe I and Fe II lines.

It is of interest to perform a similar analysis of the Ba II line at 4554 Å in the solar spectrum. In the spectrum of a star like the Sun, this line is very strong. Its core, formed in high atmospheric layers and expected to suffer serious departures from LTE, is excluded from the fitting process. This experiment, mirroring the analysis of HD 140283 and using the Fe I lines at 4602.0, 5247.1, 6151.6, 6200.3, and 6750.2 Å to find the iron abundance ($\log \epsilon(\text{Fe}) = 7.48 \pm 0.04$ dex) and FWHM (4.15 ± 0.12 km s $^{-1}$), yields a best-fit result of $\log \epsilon(\text{Ba}) = 2.32$ and $f_{\text{odd}} = 0.20$. These figures are consistent with the meteoritic abundance $\log \epsilon(\text{Ba}) = 2.22$ and isotopic fraction $f_{\text{odd}} = 0.18$. In fact, the close agreement between the derived and meteoritic f_{odd} , and the larger discrepancy for the Ba abundance, seem to confirm our expectation of a much higher accuracy in the determination of the first quantity.

In summary, our analysis of HD 140283’s Ba II 4554 Å profile gives $f_{\text{odd}} = 0.30 \pm 0.21$, a result consistent with the solar r -process contributions to barium which give

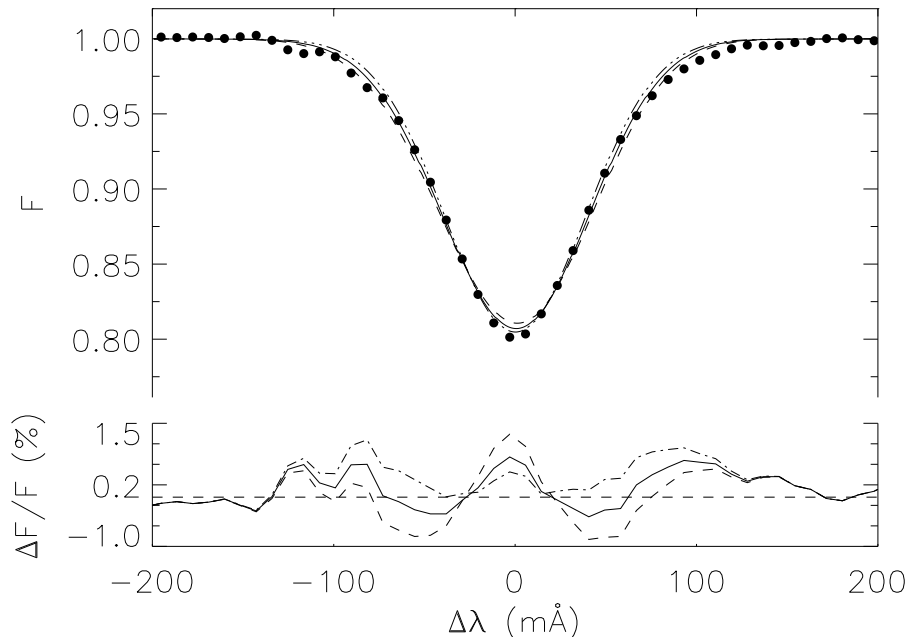


Figure 2. Best-fit ($f_{\text{odd}} = 0.31$) synthetic profile (thick solid line) and the observed profile of the Ba II 4554.0 Å line in HD 140283. The dashed and dot-dashed lines correspond to a change of ± 0.21 in f_{odd} .

$f_{\text{odd}}^r = 0.46$. Our analysis seems not to confirm Magain’s (1995) conclusion that the odd Ba isotopes have a low value ($f_{\text{odd}} = 0.06 \pm 0.06$) in the atmosphere of this star. It is clear from Figure 2 that the Ba II line profile is only weakly sensitive to f_{odd} . That is reflected in our large error bar for this parameter ($\sim 70\%$). High-resolution high-quality spectra must be paired with a realistic representation of the stellar atmosphere and the line formation to reduce the uncertainties in the isotopic fraction provided by this method.

4 NUCLEOSYNTHESIS OF HEAVY ELEMENTS

4.1 Origins of the Solar Barium Isotopes

Accurate isotopic abundances are available for the solar system from laboratory measurements on meteorites. Dissection of the heavy element abundances into s - and r -process contributions has been attempted many times with similar results. Here, we adopt Arlandini et al.’s (1999) results from their fit of predictions for the s -process operating in low mass AGB stars. We are interested in the relative abundance of the odd barium isotopes and the resolution of this quantity into s - and r -process contributions. The measured abundances give $f_{\text{odd}} = 0.18$. The r -process contributes only to ^{135}Ba , ^{137}Ba , and ^{138}Ba , and would by itself produce $f_{\text{odd}}^r = 0.46$. The s -process contributions would give $f_{\text{odd}}^s = 0.11$. (The p -nuclei ^{130}Ba and ^{132}Ba are neglected here, as is the possible but surely very small contribution of a p -process to heavier Ba isotopes.)

It is a remarkable empirical result that the relative elemental abundances of the heavier r -process products – barium and heavier – appear to be almost independent of which very metal-poor star is examined; stars enriched in s -process products are obvious exceptions. This result is highlighted

by analyses of those metal-poor stars exhibiting large r -process overabundances (Cowan et al. 1999; Westin et al. 2000; Hill et al. 2001; Cowan et al. 2001). More typical metal-poor stars also generally show a solar-like mix of the heavier elements (Burris et al. 2000; Johnson & Bolte 2001). Lighter heavier elements – Sr, Y, and Zr, for example – show some variation relative to heavier elements. Adopting the assumption that r -process products for barium and heavier elements are universal with respect to isotopic as well as elemental abundances, we expect $f_{\text{odd}} \simeq 0.5$, the solar r -process ratio, for a metal-poor star in which the r -process dominates the heavy element abundances. Theoretical estimates from r -process calculations suggest that f_{odd}^r should be accurate to 20 – 30% (Kratz & Pfeiffer 2002).

A commonly used measure of the ratio of s -process to r -process contributions to the composition of a metal-poor star is the Ba/Eu ratio. In solar system material, barium is predominantly an s -process product, and europium an r -process product: the s/r ratio for Ba is 81/19 but for Eu is 6/94 (Arlandini et al. 1999). If the r -process relative yields of barium and europium are solar-like, one expects [Ba/Eu] to approach -0.7 as the r -process dominates the composition.

4.2 HD 140283: the [Ba/Fe] and [Ba/Eu] Ratios

Although HD 140283 has been analysed frequently, abundances have been published for very few heavy elements. The reason is simply that the star is a subgiant and lines of most heavy elements are too weak for detection. We begin by considering the Ba and Eu abundances because the Ba/Eu ratio is a potent indicator of the ratio of s -process to r -process contributions to a chemical composition (see below). In Table 1, we summarise results from the literature for the LTE abundances of Fe, Sr, Y, Ba, and Eu. For [Ba/Fe], we obtain a mean [Ba/Fe] = -0.9 . The two deter-

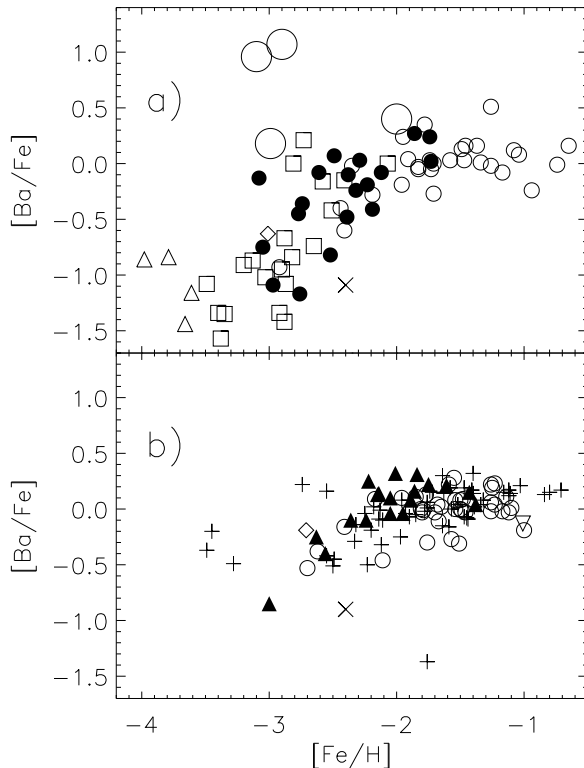


Figure 3. The abundance ratio $[\text{Ba}/\text{Fe}]$ versus $[\text{Fe}/\text{H}]$ for a representative sample of metal-poor giants (a) and dwarf/sub-giants (b). HD 140283 is identified by the large cross. The four severely r -process enriched giants are shown by large open circles. Other data points come for Figure 4a from Norris et al. (2001) - open triangles; McWilliam (1998) - open squares; Johnson & Bolte (2001) - filled circles; Fulbright (2000) - open circles; Ryan et al. (1996) - open rhombi. For Figure 4b, the data points are from Magain (1989) and Magain & Zhao (1990) - open circles; Gratton & Sneden (1994) - inverted open triangle; Ryan et al. (1996) - open rhombi; Stephens & Boesgaard (2002) - plus signs.

minations of $[\text{Eu}/\text{Fe}]$ appear to be in good agreement: the mean $[\text{Eu}/\text{Fe}] = 0.15$ with $[\text{Ba}/\text{Fe}] = -0.9$ gives $[\text{Ba}/\text{Eu}] = -1.05$. One might note that where the Eu abundance was measured, the $[\text{Ba}/\text{Eu}]$ indices are not in good agreement: $[\text{Ba}/\text{Eu}] = -0.73$ from Gratton & Sneden (1994) but -1.33 from Magain (1989) and Magain & Zhao (1990). This discrepancy may suggest that a large uncertainty be attached to the value $[\text{Ba}/\text{Eu}] = -1.05$ obtained by combining the mean $[\text{Ba}/\text{Fe}]$ from seven measurements with $[\text{Eu}/\text{Fe}]$ from two measurements.

In order to place HD 140283's Ba and Eu abundances in context, we show the variation of $[\text{Ba}/\text{Fe}]$ with $[\text{Fe}/\text{H}]$ (Figure 3) and $[\text{Ba}/\text{Eu}]$ with $[\text{Fe}/\text{H}]$ (Figure 4) for several samples of metal-poor ($[\text{Fe}/\text{H}] < -1$) stars. Stars are separated by surface gravity in giants ($\log g \leq 3.0$) and dwarfs and subgiants ($\log g > 3.0$). We include in Figures 3a and 4a the four known stars with an exceptional r -process enrichment that we mentioned in Section 4.1. A distinction by surface gravity is made because systematic errors, especially non-LTE effects, may be gravity-dependent; no obvious differences between the samples are seen in the Figures. No attempt has been made to adjust the plotted quantities for possible systematic differences between the various analyses. Where a star has been analysed more than once, we elected

to adopt the results of the analysis considered the most reliable, but the differences between investigators are small, and alternative methods of handling the duplications would not lead to different conclusions.

Figure 3 shows a well-known result (Spite & Spite 1978): $[\text{Ba}/\text{Fe}] \simeq 0$ for $[\text{Fe}/\text{H}] \geq -2$ with a decline to $[\text{Ba}/\text{Fe}] \simeq -1$ at $[\text{Fe}/\text{H}] \simeq -3$. For $[\text{Fe}/\text{H}] > -1$, extending the interval shown in Figure 3, $[\text{Ba}/\text{Fe}] \simeq 0$ (Edvardsson et al. 1993). The scatter in $[\text{Ba}/\text{Fe}]$ is particularly large for the stars with $[\text{Fe}/\text{H}] < -2$. (Stars obviously enriched in s -process products have been excluded but some stars mildly enriched may remain undetected in the samples – see below.) Viewed in Figure 3, HD 140283 has a low $[\text{Ba}/\text{Fe}]$ for its metallicity. The star at $[\text{Fe}/\text{H}] = -1.7$ with the low $[\text{Ba}/\text{Fe}]$ ($= -1.4$) is BD+80°245, a recognised α -poor star (Carney et al. 1997; Stephens & Boesgaard 2002). HD 140283 is not α -poor (Magain 1989; Gratton & Sneden 1994).

If the r -process relative yields of barium and europium are solar-like, one expects $[\text{Ba}/\text{Eu}]$ to approach -0.7 as the r -process dominates the composition. In Figure 4, we show $[\text{Ba}/\text{Eu}]$ versus $[\text{Fe}/\text{H}]$ for the same samples as plotted in Figure 3, except that a Eu abundance was not always reported in the selected references. By inspection, there is a lower bound to the points for $[\text{Fe}/\text{H}] < -2$ – see the dashed

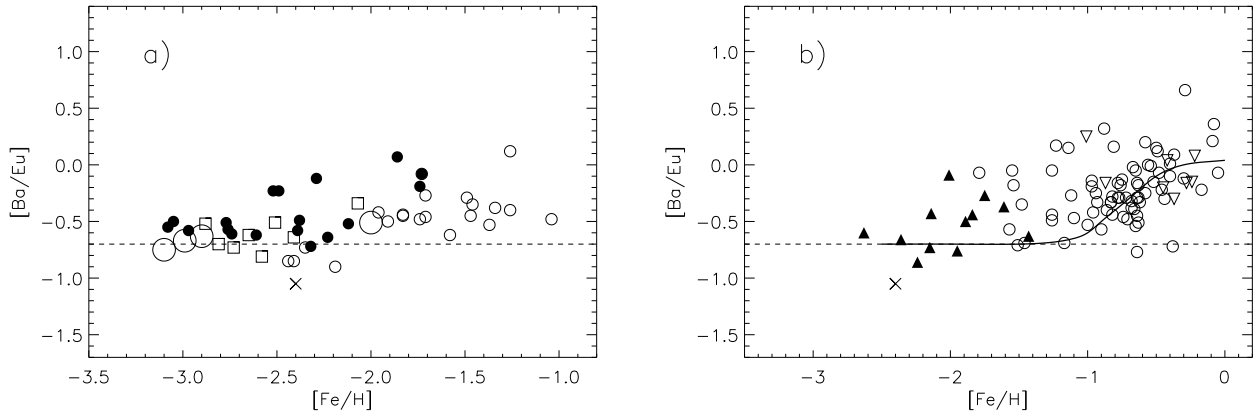


Figure 4. The abundance ratio $[\text{Ba}/\text{Eu}]$ versus $[\text{Fe}/\text{H}]$ for a representative sample of metal-poor giants (a) and dwarf/sub-giants (b). HD 140283 is identified by a cross. Symbols are as in Figure 3 where the four severely r -process enriched giants are shown by large open circles.

line at $[\text{Ba}/\text{Eu}] = -0.7$ (Figure 4), the solar r -process limit. Figure 4b shows that the lower bound to $[\text{Ba}/\text{Eu}]$ begins to rise at $[\text{Fe}/\text{H}] \simeq -1$ (see the solid line in Figure 4b) to match the solar ratio ($\equiv 0$) at $[\text{Fe}/\text{H}] \simeq 0$ (Edvardsson et al. 1993; Woolf, Tomkin, & Lambert 1995; Koch & Edvardsson 2002).*

If Gratton & Sneden’s (1994) estimate of $[\text{Ba}/\text{Eu}]$ ($\simeq -0.7$) is adopted, HD 140283 has the $[\text{Ba}/\text{Eu}]$ ratio expected of the r -process. If $[\text{Ba}/\text{Eu}] = -1.3$, as Magain’s (1989, also Magain & Zhao 1990) analysis suggests, HD 140283 has an unusually low $[\text{Ba}/\text{Eu}]$ ratio. At our adopted $[\text{Ba}/\text{Eu}] = -1.05$, HD 140283 appears to fall below the lower bound for the r -process as set empirically by the four heavily r -process enriched and other stars, but improved measurements of Eu II (and other) lines in HD 140283 would be welcomed. Note in Figure 4b that Magain’s results for other stars tend to $[\text{Ba}/\text{Eu}] \sim -0.7$, and, therefore, his result for HD 140283, a similar star to the rest of his sample, may be correct. Magain’s (1989) measurement of $[\text{La}/\text{Eu}]$ is consistent within the uncertainties with the r -process expectation. No other elements heavier than barium have been measured in HD 140283. Given this evidence, we may consider it likely that the barium in HD 140283’s atmosphere was produced via the r -process with a solar r -like mix of the heavier elements.

4.3 HD 140283: $[\text{Sr}/\text{Ba}]$ and $[\text{Y}/\text{Ba}]$ Ratios

Equivalence between relative abundances of heavy elements in metal-poor stars and the solar system r -process abundances does not extend to elements lighter than barium. In Figure 5, we show $[\text{Sr}/\text{Ba}]$ and $[\text{Y}/\text{Ba}]$ versus $[\text{Fe}/\text{H}]$ for metal-poor stars. It is known (McWilliam et al. 1995a, b; McWilliam 1998) that Sr and Y abundances span a much

larger range than do the abundances of Ba and heavier elements at a given $[\text{Fe}/\text{H}]$. Figure 5 shows clearly (McWilliam 1998) that there is a lower bound and also suggests that there is an upper envelope to $[\text{Sr}/\text{Ba}]$ and $[\text{Y}/\text{Ba}]$. For $[\text{Fe}/\text{H}] > -1$, the lower bound and the upper envelope converge and tend to $[\text{Sr}/\text{Ba}] = [\text{Y}/\text{Ba}] = 0$. The upper envelopes in Figure 5 appear to increase with decreasing $[\text{Fe}/\text{H}]$, but present data would allow for a levelling off for $[\text{Fe}/\text{H}] < -3$. The quartet of stars very strongly enriched in heavy elements sit at or close to the lower bounds, which are slightly below those expected by removing the *main s*-process (the contribution from AGB stars) from the solar abundances: $[\text{Sr}/\text{Ba}] = -0.1$ and $[\text{Y}/\text{Ba}] = -0.4$. The small differences are likely due to the fact that Sr and Y in the solar mix receive a contribution from the *weak s*-process (the contribution from massive stars) which is also reduced in the case of metal-poor stars.

HD 140283 sits in Figure 5 close to the upper envelopes for its $[\text{Fe}/\text{H}]$. The observation that many metal-poor stars have $[\text{Sr}/\text{Ba}]$ and $[\text{Y}/\text{Ba}]$ ratios in excess of the lower bound is part of the evidence that has led to suggestions that there are multiple sites for the r -process (Wasserburg, Busso, & Gallino 1996; Qian & Wasserburg 2001; Sneden et al. 2000). In particular, Qian & Wasserburg (2001) explore a scenario involving three sources of heavy elements: (i) a pre-Galactic or ‘prompt’ component of low metallicity ($[\text{Fe}/\text{H}] \sim -3$) contributing Sr, Y, and Zr, (ii) a common type of supernova providing heavy elements Sr to Ba to U in solar r -process ratios with smaller relative abundances for the elements lighter than barium, and (iii) a rarer type of supernova contributing iron, the lighter of the heavy elements, and possibly some barium. In such a composite picture, the stars with $[\text{Fe}/\text{H}] \sim -3$ were formed from pre-Galactic gas to which a common supernova or two added its ejecta. Qian & Wasserburg’s recipe matches HD 140283’s abundances satisfactorily when ejecta of 3 common supernovae are mixed with the pre-Galactic gas. In this mix, the bulk of the Sr and Y are provided by the prompt material, and the Ba and Eu by the common supernovae.

Strontium and Y (also Zr) abundances in HD 140283 show that these lighter elements do not have the pattern

* Two stars from Fulbright’s (2000) sample extend the lower bound to about $[\text{Fe}/\text{H}] = -0.5$. Close spectroscopic scrutiny of this pair is warranted in order to confirm the apparent dominance of the r -process at this high metallicity; Fulbright measured only Ba and Eu among the set of heavier elements.

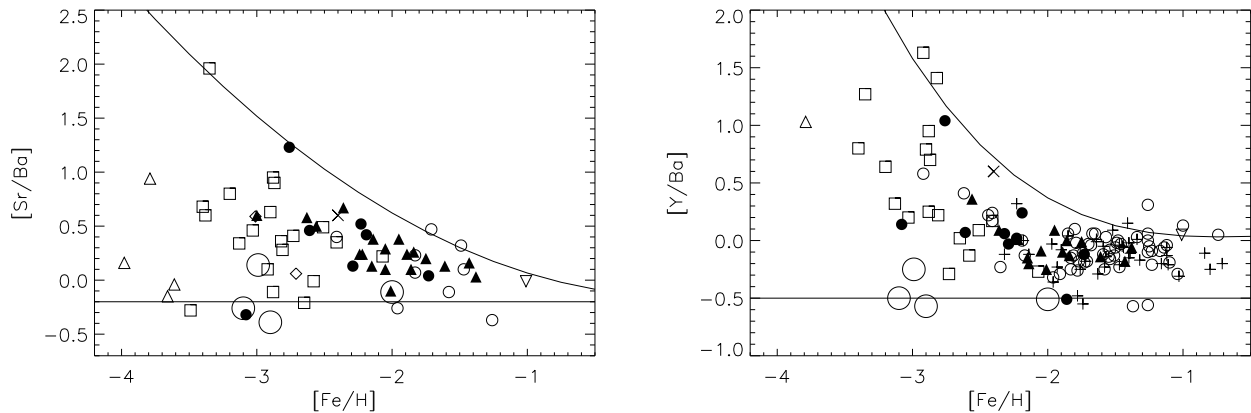


Figure 5. The abundance ratios $[\text{Sr}/\text{Ba}]$ and $[\text{Y}/\text{Ba}]$ versus $[\text{Fe}/\text{H}]$ for representative samples of metal-poor giants and dwarfs. As before, HD 140283 is identified by the large cross, the four severely r -process enriched giants by the large open circles, and the other symbols are explained in Figure 3. The solid lines sketch the possible boundaries to the points.

of the solar r -process. In sharp contrast, those stars most heavily enriched in r -process products do have Sr and Y abundances (relative to Ba) that are quite similar to solar r -process fractions. Whether this difference between HD 140283 and the purest samples of r -process products should affect the expected barium isotopic mixture is unclear.

4.4 The Barium Isotopic Ratio in other Metal-Poor Stars

Magain’s method of determining f_{odd} from the width of the 4554 Å line has, so far as we are aware, not been applied to other metal-poor stars. An alternative method was introduced by Magain & Zhao (1993b) for stars somewhat more metal-rich than HD 140283. Cowley & Frey (1989) had earlier discussed this approach to an isotopic analysis. In this procedure, the Ba abundance is derived from the 4554 Å and also from at least one of the excited lines at 5853 Å, 6142 Å, and 6496 Å. The abundance derived from an excited line in a metal-poor star is independent of the isotopic and hyperfine splitting; the splittings are too small to affect these lines. In appropriate stars, the much stronger 4554 Å line will be saturated, and, hence, the equivalent width is sensitive to the isotopic and hyperfine splitting, that is to f_{odd} . Then, f_{odd} follows by requiring that the resonance line give the same total Ba abundance as the excited lines.

In an initial application to four stars with $[\text{Fe}/\text{H}] \sim -2$, Magain & Zhao (1993b) found a mean value for f_{odd} close to the prediction from the solar r -process. Mashonkina & Gehren (2000) analysed about 20 stars using their non-LTE calculations of the Ba II lines. The abundance difference between the 4554 Å line and excited lines was calculated for two isotopic mixtures: the solar mix ($f_{\text{odd}} = 0.18$), and the solar r -process mix ($f_{\text{odd}} = 0.46$). For stars with $-2 \leq [\text{Fe}/\text{H}] \leq -0.5$ for which the method is useful, the abundance from the 4554 Å line was generally more consistent with that from the excited lines when the r -process and not the solar isotopic mix was assumed: the abundance difference was only about 0.1 dex between predictions for the two isotopic mixtures. The $[\text{Ba}/\text{Eu}]$ and $[\text{Sr}/\text{Ba}]$ ratio for most of the stars are close to the r -process limiting values:

Mashonkina & Gehren give these ratios for some stars, and for others we obtain them from Fulbright (2000). For such a sample, the r -process isotopic mix is not an unexpected result. Earlier, Mashonkina, Gehren, & Bikmaev (1999) applied the method to a star with $[\text{Fe}/\text{H}] = -2.2$ of unknown $[\text{Ba}/\text{Eu}]$ with a normal $[\text{Sr}/\text{Ba}]$ ($= -0.18$) for which a solar mix of the isotopes was found. This method is sensitive to atmospheric effects such as the microturbulence, line broadening, and departures from LTE, as Cowley & Frey (1989) had noted.

4.5 Cosmic Scatter in the s to r Ratio for Metal-poor Stars?

Although the scatter in $[\text{Ba}/\text{Eu}]$ at a fixed (low) $[\text{Fe}/\text{H}]$ is much less than displayed by either $[\text{Ba}/\text{Fe}]$ or $[\text{Eu}/\text{Fe}]$, there appear to be metal-poor stars with $[\text{Ba}/\text{Eu}]$ above the lower bound by more than the supposed errors. A simple way to give a star a high $[\text{Ba}/\text{Eu}]$ for a given $[\text{Fe}/\text{H}]$ is to enrich it in s -process products.[†] The s -process enriched material may have been present in the natal clouds, or accreted by passage through an interstellar cloud with a higher than average abundance of s -process products. Alternatively, the s -process products may have been transferred from a companion, as occurs in the classical Barium and CH stars. Contamination of some stars by s -process products was suggested earlier in our discussion of Mg isotopic ratios in metal-poor stars (Gay & Lambert 2000). (There is too the possibility that the He-core flash in a low mass giant may trigger neutron release and synthesis of heavy elements. Such an event is unlikely to provide a solar-like mix of the elements. If the core flash is responsible for the differences in $[\text{Ba}/\text{Eu}]$ ratios, giants but not dwarfs should show this effect. Figure 4 seems to contradict this idea.)

Natal clouds with differing compositions are thought to be responsible for the spread in heavy r -process elemental

[†] The few known very metal-poor analogues of the Barium stars and other examples of markedly s -process enriched stars have been excluded from Figures 3 and 4.

abundances between stars of a common very low $[\text{Fe}/\text{H}]$. As shown in Fig. 1, scatter decreases with increasing $[\text{Fe}/\text{H}]$ as the number of r -process contributors grows. As long as the relative yields of Ba and Eu from the r -process are the same for all contributing Type II supernovae, if the only production mechanism is the r -process, $[\text{Ba}/\text{Eu}]$ will show no scatter. That could be the case in Fig. 4 for the lowest $[\text{Fe}/\text{H}]$. Donors of s -products are surely more slowly evolving than the supernovae contributing r -process products. Clouds first contaminated with s -products may form stars of similar $[\text{Fe}/\text{H}]$ but differing $[\text{Ba}/\text{Eu}]$. Onset of this scatter is expected at a $[\text{Fe}/\text{H}]$ greater than that marking the onset of r -process scatter, i.e., the minimum observed $[\text{Fe}/\text{H}]$ ($\simeq -4$). This speculation is consistent with the data plotted in Figure 4.

If our suggestion about s -process contamination causing the scatter in $[\text{Ba}/\text{Eu}]$ is correct, other heavy elements with an s -process contribution should show a scatter correlated with the enhancement of $[\text{Ba}/\text{Eu}]$ above the lower bound. This idea is tested in Figure 7 using Johnson & Bolte’s data. Figure 7 appears to show that stars with $[\text{Ba}/\text{Eu}]$ in excess of the r -process lower bound are also overabundant in other (s -process dominated) heavy elements. We note that the trail of data points in the various panels commences from about the expected and well-populated endpoint for the solar r -process ratios. The apparent trends seem to favour our hypothesis. Unfortunately, a dysprosium abundance was provided by Johnson & Bolte for just one of the six ‘Ba-rich’ ($[\text{Ba}/\text{Eu}] > -0.3$) stars. Burris et al. give Dy abundances for an additional two ‘Ba-rich’ stars which at $[\text{Dy}/\text{Eu}] = -0.07$ and 0.11 indicate, as required by our speculation, that Dy is not enriched in the ‘Ba-rich’ stars. However, we must recognize that the Dy abundances of the stars with $[\text{Ba}/\text{Eu}]$ at the r -process value show a large spread presumably reflecting measurement errors for this element. Perhaps, our suggestion about the onset of the s -process as a contributor to the scatter in relative abundances will stimulate the pursuit of a higher accuracy in the abundance determinations of these heavy elements.

5 CONCLUDING REMARKS

Our profile analysis of the Ba II 4554 Å line does not confirm Magain’s (1995) result that the mix of odd to even isotopes, f_{odd} , is not the high value ($\simeq 0.5$) expected of the r -process on the assumption that the r -process always provides a solar r -process mix of heavy nuclides. On the contrary, our estimate of f_{odd} is compatible with a solar r -process mix of the barium isotopes.

Magain argued also that the then available data on the abundances of heavy elements in metal-poor stars did not support the view that the r -process contributions were dominant, and, thus, his measurement of a low value for f_{odd} was not at odds with his view of the pattern of elemental abundances. In striking contrast, the evidence now available shows that the abundances for heavy elements in metal-poor stars are in general reflective of an r -process with yields for barium and heavier elements remarkably similar to the solar case. Although a thorough analysis of the heavier elements present in HD 140283’s atmosphere has yet to be presented, it seems likely that a solar-like r -process mix is present.

Then, it is not surprising that the barium isotopic mix is similar to that of the solar r -process fraction of barium.

Extensive and accurate work on the neutron capture cross-sections for barium isotopes has enabled f_{odd}^s and, hence, f_{odd}^r to be determined accurately (Arlandini et al. 1999). More directly, analyses of the stars with extreme enrichments of the r -process products give a Ba/Eu ratio consistent with the estimated solar r -process fractions. That the solar r -process pattern of elemental abundances fits the abundances of barium and heavier elements in metal-poor stars is a remarkable empirical fact. Sneden et al. (2002) have shown that the europium isotopic abundances in the heavily r -process enriched metal-poor stars have their solar r -process ratio. There remains the observation that the Sr/Ba and Y/Ba ratios of metal-poor stars often exceed that expected of the r -process and observed in those heavily r -process enriched stars. As Figure 5 shows, HD 140283 seems to be among the stars with the greatest Sr/Ba and Y/Ba ratios. For this and similar stars, the Sr and Y may have been provided by the pre-Galactic gas (Qian & Wasserburg 2001). Can this material harbor distinct isotopic mixtures for barium and other elements, especially Sr, Y, and Zr?

Our analysis clearly shows that the barium isotopic mixture has a rather subtle effect on the 4554 Å profile. High-resolution spectra of high S/N ratio are just one prerequisite for a determination of f_{odd} . With today’s large telescopes and the development of hydrodynamical model atmospheres, it may be possible to refine and extend the isotopic analyses to other metal-poor stars and to other elements.

6 ACKNOWLEDGMENTS

We are indebted to Ramón J. García López for obtaining part of the observations used in this work. We thank Chris Sneden and John Cowan for helpful discussions. NSO/Kitt Peak FTS data used here were produced by NSF/NOAO. This research was supported in part by the National Science Foundation (grant AST-0086321) and the Robert A. Welch Foundation of Houston, Texas (grant F-634).

REFERENCES

- Allende Prieto, C. 1998, PhD Thesis, Univ. of La Laguna
- Allende Prieto, C., García López, R. J., Lambert, D. L., & Gustafsson, B. 1999, ApJ, 526, 991
- Allende Prieto, C., Ruiz Cobo, B., & García López, R. J. 1998, ApJ, 502, 951
- Arlandini, C., Käppeler, F., Wisshak, K., Gallino, R., Lugaro, M., Busso, M., & Straniero, O. 1999, ApJ, 525, 886
- Barklem, P. S., & O’Mara, B. J. 1997, MNRAS, 290, 102
- Barklem, P. S., Piskunov, N., & O’Mara, B. J. 2000, A&AS, 142, 467
- Blackwell, D.E., Booth, A.J., Haddock, D.J., Petford, A.D., & Leggett, S.K. 1986, MNRAS, 220, 549
- Burris, D. L., Pilachowski, C. A., Armandroff, T. E., Sneden, C., Cowan, J. J., & Roe, H. 2000, ApJ, 544, 302
- Carney, B.W., Wright, J.S., Sneden, C., Laird, J.B., Aguilar, L.A., & Latham, D.W. 1997, AJ, 114, 363
- Cowan, J. J., Pfeiffer, B., Kratz, K.-L., Thielemann, F.-K., Sneden, C., Burles, S., Tytler, D., & Beers, T. C. 1999, ApJ, 521, 194

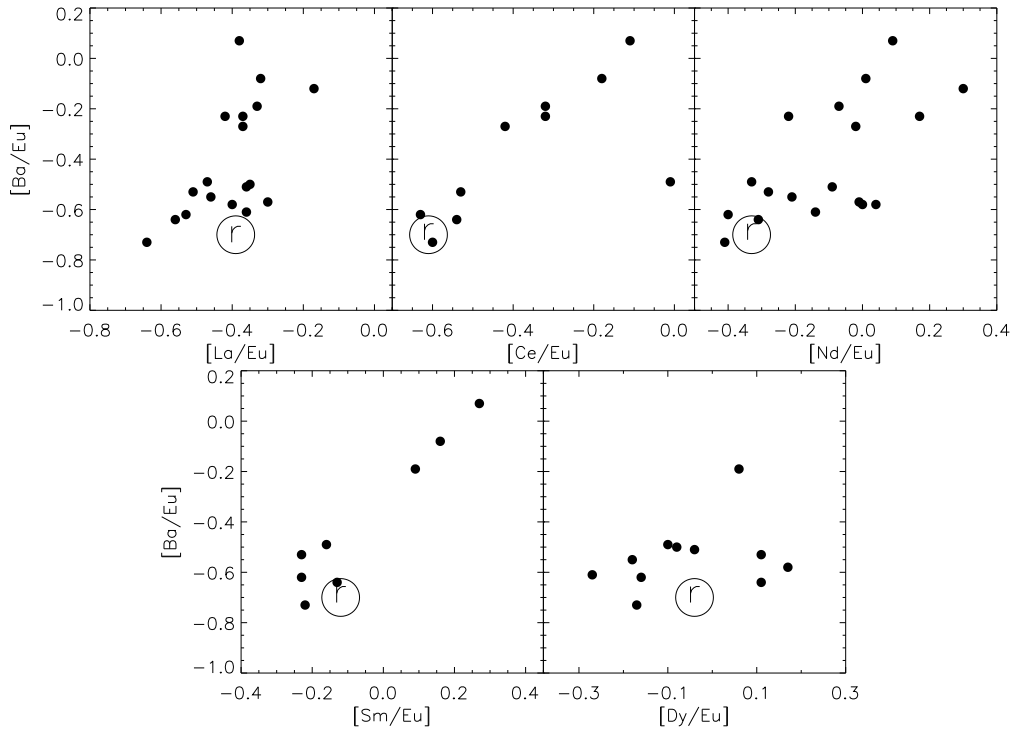


Figure 6. The abundance ratio $[Ba/Eu]$ versus $[X/Eu]$, where X is La, Ce, Nd, Sm, and Dy, for giants analysed by Johnson & Bolte (2001). The solar r -process ratio is indicated in each panel by the circled- r .

- Cowan, J. J., Sneden, C., Burles, S., Ivans, I. I., Beers, T. C., Truran, J. W., Lawler, J. E., Primas, F., Fuller, G. M., Pfeiffer, B., & Kratz, K.-L. 2001, *ApJ*, submitted
- Cowley, C. R. & Frey, M. 1989, *ApJ*, 346, 1030
- Edvardsson, B., Andersen J., Gustafsson, B., Lambert, D.L., Nissen, P.E., & Tomkin, J. 1993, *A&A*, 275, 101
- Fulbright, J.P. 2000, *AJ*, 120, 1841
- Gay, P.L., & Lambert, D.L. 2000, *ApJ*, 533, 260
- Gehren, T., Butler, K., Mashonkina, L., Reetz, J., & Shi, J. 2001, *A&A*, 366, 981
- Giridhar, S. & Arellano Ferro, A. 1994, *Rev. Mexicana Astron. Astrofis.*, 29, 214
- Gratton, R. G. & Sneden, C. 1994, *A&A*, 287, 927
- Hill, V., Plez, B., Cayrel, R., & Beers, T.C. 2001, *ASP Conf. Ser.*, 245, 316
- Johnson, J.A., & Bolte, M. 2001, *ApJ*, 554, 888
- Koch, A., & Edvardsson, B. 2002, *A&A*, 381, 500
- Kratz, K.-L., & Pfeiffer, B. 2002, *MPI für Astrophysik Rept.* MPA/P13, 67
- Kurucz, R. L. 1992, private communication
- Kurucz, R. L., Furenlid, I. & Brault, J. 1984, *National Solar Observatory Atlas, Sunspot*, New Mexico: National Solar Observatory, 1984,
- Magain, P. 1989, *A&A*, 209, 211
- Magain, P. 1995, *A&A*, 297, 686
- Magain, P., & Zhao, G. 1990, *A&A*, 238, 242
- Magain, P. & Zhao, G. 1993a, *A&A*, 268, L27
- Magain, P. & Zhao, G. 1993b, in *Origin and Evolution of the Elements*, ed. N. Prantzos et al., (Cambridge: Cambridge Univ. Press), 480
- Mashonkina, L. & Gehren, T. 2000, *A&A*, 364, 249
- Mashonkina, L., Gehren, T., & Bikmaev, I. 1999, *A&A*, 343, 519
- McWilliam, A. 1998, *AJ*, 115, 1640
- McWilliam, A., Preston, G. W., Sneden, C., & Searle, L. 1995a, *AJ*, 109, 2736
- McWilliam, A., Preston, G. W., Sneden, C., & Searle, L. 1995b, *AJ*, 109, 2757
- Mishenina, T.V., & Kovtyukh, Y.V. 2001, *A&A*, 370, 951
- Nelder, J. A., & Mead, R., *Computer Journal*, 7, 308
- Norris, J.E., Ryan, S.G., & Beers, T.C. 2001, *ApJ*, 561, 1034
- O'Brian, T. R., Wickliffe, M. E., Lawler, J. E., Whaling, W., & Brault, J. W. 1991, *JOSA B*, 8, 1185
- Press, W. H., Flannery, B. P., Teukolsky, S. A., & Vetterling, W. T. 1988, *Numerical Recipes in C* (Cambridge: Cambridge Univ. Press)
- Qian, Y.-Z., & Wasserburg, G.J. 2001, *ApJ*, 559, 925
- Rutten, R. J. 1978, *Sol. Phys.*, 56, 237
- Ryan, S.G., Norris, J.E., & Beers, T.C. 1996, *ApJ*, 471, 254
- Ryan, S.G., Gregory, S. G., Kolb, U., Beers, T. C., & Toshitaka, K. 2002, *ApJ*, in press (astro-ph/0202369)
- Sneden, C. 1973, PhD Thesis, Univ. of Texas at Austin
- Sneden, C., Cowan, J.J., Ivans, I.I., Fuller, G.M., Burles, S., Beers, T.C., & Lawler, J.E. 2000, *ApJ*, 533, L139
- Sneden, C., Cowan, J.J., Lawler, J.E., Burles, S., Beers, T.C., & Fuller, G.M. 2002, *ApJ*, 566, L25
- Snider, S., Allende Prieto, C., von Hippel, T., Beers, T. C., Sneden, C., Qu, Y., & Rossi, S. 2001, *ApJ*, 562, 528
- Spite, F., & Spite, M. 1978 *A&A*, 67, 23
- Stephens, A., & Boesgaard, A.M. 2002, *AJ*, in press
- Thévenin, F., & Idiart, T.P. 1999, *ApJ*, 521, 753
- Truran, J. W. 1981, *A&A*, 97, 391
- Tull, R. G., MacQueen, P. J., Sneden, C., & Lambert, D. L. 1995, *PASP*, 107, 251
- Wasserburg, G.J., Busso, M., & Gallino, R. 1996, *ApJ*, 529, L21
- Westin, J., Sneden, C., Gustafsson, B., & Cowan, J.J. 2000, *ApJ*, 530, 783
- Woolf, V. M., Tomkin, J., & Lambert, D. L. 1995, *ApJ*, 453, 660